Higher Donor Excited States for Prolate-Spheroid Conduction Bands: A Reevaluation of Silicon and Germanium

R. A. FAULKNER
Bell Telephone Laboratories, Murray Hill, New Jersey 07974
(Received 9 October 1968; revised manuscript received 10 March 1969)

An extension of the Kohn–Luttinger method for the energy levels of the effective-mass Hamiltonian $H=(P_x^2/2m_\perp+P_y^2/2m_\perp+P_z^2/2m_{||})-e^2/Kr$ is made via the Rayleigh–Ritz approach. The method is capable of indefinite extension provided one is prepared to deal with large matrices. The first nine S-like energy levels and the first eighteen P-like energy levels are presented here as a function of the mass ratio $\gamma=m_\perp/m_{||}$ for $0<\gamma\leq 1$. The experimental results for the P-like excited states of silicon and germanium can be fitted to within experimental error if one takes the low-temperature static dielectric constant of silicon to be 11.40 ± 0.05, and that of germanium to be 15.36 ± 0.05. The situation concerning donor levels in GaP is discussed briefly.

I. INTRODUCTION

SINCE the original theoretical work[1,2] on donor states in silicon and germanium in 1954–1955, substantial experimental information has been gained on the energy levels of the excited P-like states in these materials.[3–9] Cyclotron-resonance work[10,11] has yielded effective-mass values accurate to 0.1%. These experimental developments have outstripped the theory in precision. In this paper, theory catches up.

The method of calculation of the energy levels of a donor in a material having a prolate-spheroid conduction band, such as Si or Ge, is presented in Sec. II. The numerical results are presented in Sec. III and a reevaluation of the experimental spectra of Si and Ge is made in Sec. IV. The situation concerning donor levels in GaP is also discussed in Sec. IV.

II. ENERGY LEVELS OF THE EFFECTIVE-MASS HAMILTONIAN

In the effective-mass approximation, the energy levels of donors in a material having a conduction-band minimum in the shape of a prolate spheriod (either one or several equivalent minima) are given by the solutions of a Schrödinger equation with the Hamiltonian

$$H_0=-\frac{\hbar^2}{2m_\perp}\left(\frac{\partial^2}{\partial x^2}+\frac{\partial^2}{\partial y^2}\right)-\frac{\hbar^2}{2m_{||}}\frac{\partial^2}{\partial z^2}-\frac{e^2}{Kr}, \quad (2.1)$$

where K is the dielectric constant.

Following Kohn and Luttinger,[2] if we take the units of length and energy to be, respectively,

$$a_B=\hbar^2K/m_\perp e^2; \quad \text{and} \quad \epsilon_0=m_\perp e^4/2\hbar^2K^2, \quad (2.2)$$

we are led to the dimensionless Hamiltonian

$$H_1=-\left(\frac{\partial^2}{\partial x^2}+\frac{\partial^2}{\partial y^2}+\gamma\frac{\partial^2}{\partial z^2}\right)-\frac{2}{r}, \quad (2.3)$$

where $\gamma=m_\perp/m_{||}$ is the mass ratio.

The method used in this paper to find the lowest few eigenvalues of H_1 is the Rayleigh-Ritz method,[12] wherein N orthonormal functions ϕ_j are used to set up an $N\times N$ Hermitian matrix:

$$H_{j',j}=\int d^3x\,\phi_{j'}^*(\mathbf{x})H_1\phi_j(\mathbf{x}) \quad (2.4)$$

whose eigenvalues are upper bounds to the lowest N eigenvalues of H_1. It is important to emphasize that the method yields upper bounds because the solutions are functions of nonlinear variational parameters which may be varied independently to find the lowest upper bound for each eigenvalue. The choice of parameters which minimizes an upper bound to one eigenvalue does not necessarily minimize an upper bound to a different eigenvalue.

A convenient set of orthonormal functions to use is the set

$$\phi_{nlm}(x,y,z)=(\beta/\gamma)^{1/4}\psi_{nlm}(x,y,(\beta/\gamma)^{1/2}z), \quad (2.5)$$

where $\psi_{nlm}(x,y,z)$ are normalized hydrogenic wave functions

$$\psi_{nlm}(x,y,z)=R_{nl}(r)Y_{lm}(\theta,\phi), \quad (2.6)$$

and β is an adjustable parameter.

$Y_{lm}(\theta,\phi)$ is a normalized spherical harmonic corresponding to orbital angular momentum l and projection of angular momentum m.

[1] C. Kittel and A. H. Mitchell, Phys. Rev. **96**, 1488 (1954).
[2] W. Kohn and J. M. Luttinger, Phys. Rev. **98**, 915 (1955).
[3] J. W. Bichard and J. C. Giles, Can. J. Phys. **40**, 1480 (1962).
[4] W. E. Krag and H. J. Zeiger, Phys. Rev. Letters **8**, 485 (1962).
[5] J. H. Reuszer and P. Fisher, Phys. Rev. **135**, A1125 (1964).
[6] R. L. Aggarwal and A. K. Ramdas, Phys. Rev. **137**, A602 (1965).
[7] R. L. Aggarwal, P. Fisher, V. Mourzine, and A. K. Ramdas, Phys. Rev. **138**, A882 (1965).
[8] J. H. Reuszer and P. Fisher, Phys. Rev. **140**, A245 (1965).
[9] R. L. Aggarwal and A. K. Ramdas, Phys. Rev. **140**, A1246 (1965).
[10] B. W. Levinger and D. R. Frankl, J. Phys. Chem. Solids **20**, 281 (1961).
[11] J. C. Hensel, H. Hasegawa, and M. Nakayama, Phys. Rev. **138**, A225 (1965).

[12] There are many good treatments of the Rayleigh-Ritz method in textbooks on mathematical methods. See, for example, G. Goertzel and N. Tralli, *Some Mathematical Methods of Physics* (McGraw-Hill Book Co., New York, 1960).

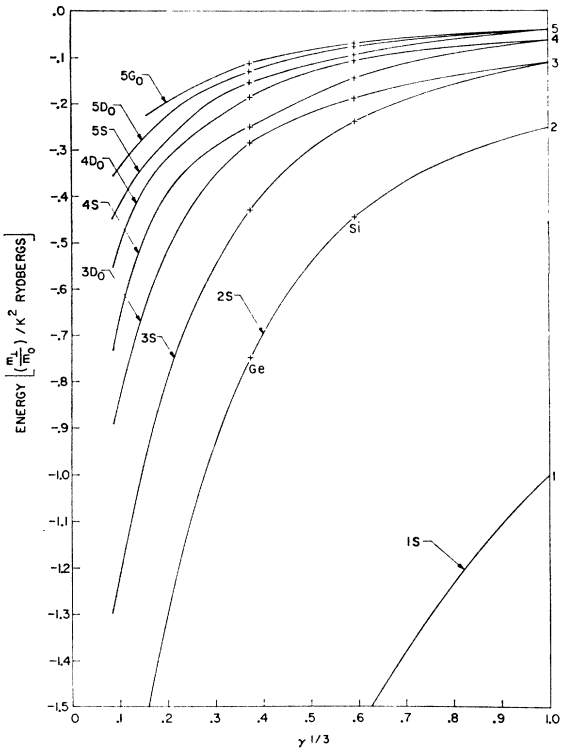

FIG. 1. S-like donor energy levels calculated in the effective mass approximation as functions of the mass ratio $\gamma=m_\perp/m_\parallel$. The energy unit is $m_\perp e^4/2\hbar^2K^2$.

The normalized radial wave function corresponding to principal quantum number n and angular momentum l is[13]

$$R_{nl}(r)=\frac{2\alpha^{3/2}}{n^2}\left(\frac{(n-l-1)!}{[(n+l)!]^3}\right)^{1/2}\left(\frac{2\alpha r}{n}\right)^l \times e^{-\alpha r/n}L_{n-l-1}^{2l+1}(2\alpha r/n), \quad (2.7)$$

and the Laguerre polynomial is

$$L_p^k(z)=\sum_{s=0}^{p}(-1)^s\frac{[(p+k)!]^2}{(p-s)!(k+s)!s!}z^s. \quad (2.8)$$

The members of the set of functions (2.5) are orthogonal for different values of (l,m) because of the angular part. They are orthogonal for different n but the same (l,m) because of the radial part. Therefore, we may consider the parameter α appearing in (2.7) to be a variational parameter which is the same for all functions of the same (l,m) but different n:

$$R_{nl}(r)=R_{nl}(\alpha(l,m);r). \quad (2.9)$$

[13] The notation and conventions used here for the hydrogenic wave functions corresponds to that used by A. Messiah, in *Quantum Mechanics* (North-Holland Publishing Company, Amsterdam, 1961), Vol. I. See Appendix B of this reference.

Using the set of functions (2.5), we write the Hamiltonian matrix

$$\langle n'l'm'|H|nlm\rangle$$
$$=\int d^3x\left(\frac{\beta}{\gamma}\right)^{1/2}\psi_{n'l'm'}^*\left(x,y,\left(\frac{\beta}{\gamma}\right)^{1/2}z\right)\times\left[-\left(\frac{\partial}{\partial x^2}+\frac{\partial^2}{\partial y^2}+\gamma\frac{\partial^2}{\partial z^2}\right)-\frac{2}{r}\right]\times\psi_{nlm}\left(x,y,\left(\frac{\beta}{\gamma}\right)^{1/2}z\right)$$
$$=\int d^3x\psi_{n'l'm'}^*(x,y,z)\left[-\left(\frac{\partial^2}{\partial x^2}+\frac{\partial^2}{\partial y^2}+\frac{\partial^2}{\partial z^2}\right)+(1-\beta)\frac{\partial^2}{\partial z^2}-\frac{2}{[x^2+y^2+(\gamma/\beta)z^2]^{1/2}}\right]\psi_{nlm}(x,y,z)$$
$$=\delta_{mm'}[\delta_{ll'}T_{n'n}(l,m)+V^{(1)}{}_{n'l';nl}(m)+V^{(2)}{}_{n'l';nl}(m)], \quad (2.10)$$

where

$$T_{n'n}(l,m)=-\int_0^\infty dr\, rR_{n'l}(\alpha(l,m);r)\times\frac{\partial^2}{\partial r^2}rR_{nl}(\alpha(l,m);r), \quad (2.11)$$

$$V^{(1)}{}_{n'l';nl}(m)=(1-\beta)\int d^3x\,\psi_{n'l'm}^*(\mathbf{x})\times\frac{\partial^2}{\partial z^2}\psi_{nlm}(\mathbf{x}), \quad (2.12)$$

$$V^{(2)}{}_{n'l';nl}(m)=-2\int d^3x\frac{\psi_{n'l'm}^*(\mathbf{x})\psi_{nlm}(\mathbf{x})}{[x^2+y^2+(\gamma/\beta)z^2]^{1/2}}. \quad (2.13)$$

The Hamiltonian H_1 is invariant under the operations of parity and of rotation about the z axis. It cannot therefore mix states of different parity or different projection of angular momentum.

The term $T_{n'n}(l,m)$ will mix states of the same (l,m) but different n. The second term, $V^{(1)}$, will mix states of different n and only those states for which $l'=l$ or $l'=l\pm2$. The third term will mix all states of different n and such that $l'=l\pm2j$, $j=0, 1, 2, \cdots$.

Because different values of m are never mixed, we shall drop the explicit dependence of quantities on m in most of the remainder of this section.

Let us define the following functions:

$$I(l',l)=\int d\Omega\frac{Y_{l'm}^*(\Omega)Y_{lm}(\Omega)}{[1-(1-\gamma/\beta)\cos^2\theta]^{1/2}}, \quad (2.14)$$

$$J^{(0)}(n',l';n,l)=\int_0^\infty dr\, R_{n'l'}(\alpha(l'),r)R_{nl}(\alpha(l),r), \quad (2.15)$$

$$J^{(1)}(n',l';n,l)=\int_0^\infty dr\, rR_{n'l'}(\alpha(l'),r)R_{nl}(\alpha(l),r), \quad (2.16)$$

$$J^{(2)}(n',l';n,l)=\int_0^\infty dr\, r^2R_{n'l'}(\alpha(l'),r)R_{nl}(\alpha(l),r), \quad (2.17)$$

$$D(n',l';n,l)=\int_0^\infty dr\, R_{n'l'}(\alpha(l'),r)r\frac{\partial}{\partial r}R_{nl}(\alpha(l),r). \quad (2.18)$$

Straightforward but tedious operations with Clebsch-Gordan coefficients and the properties of the R_{nl} yield the Hamiltonian matrix: for $l'=l$,

$$H(n'l;n,l)=-2I(l,l)J^{(1)}(n',l;n,l)+\left\{1-(1-\beta)\frac{1}{3}\left[1+\frac{2l(l+1)-6m^2}{(2l-1)(2l+3)}\right]\right\}\times\left[-\delta_{n',n}\frac{\alpha^2(l)}{n^2}+2\alpha(l)J^{(1)}(n',l;n,l)\right]; \quad (2.19)$$

for $l'=l-2$,

$$H(n',l-2;n,l)=-2I(l-2,l)J^{(1)}(n',l-2;n,l)+(1-\beta)\frac{1}{(2l-1)}\left[\frac{(l^2-m^2)[(l-1)^2-m^2]}{(2l+1)(2l-3)}\right]^{1/2}\times\left\{\frac{1}{2}\left[\frac{\alpha^2(l)}{n^2}+\frac{\alpha^2(l-2)}{n'^2}\right]J^{(2)}(n',l-2;n,l)-[\alpha(l)+\alpha(l-2)]J^{(1)}(n',l-2;n,l)+l(2l-1)J^{(0)}(n',l-2;n,l)+(2l-1)D(n',l-2;n,l)\right\}; \quad (2.20)$$

for $l'=l\pm 2j$; $j\neq 0, 1$,

$$H(n',l';n,l)=-2I(l',l)J^{(1)}(n'l';n,l). \quad (2.21)$$

Equations (2.19), (2.20), and (2.21) can be used to set up a Hamiltonian matrix of any desired order. Using the formulas (2.7) and (2.8), the functions $J^{(0)}$, $J^{(1)}$, $J^{(2)}$, and D can be expressed analytically for all values of n', n, l', and l. All that is left is the formula for $I(l',l)$ for all values of l' and l (and m). This author did not find a way to express the general formula for $I(l',l)$, and contented himself with evaluating it for the specific values of l, l' and m actually used in the numerical computation.

Having set up the Hamiltonian matrix to the desired order, the eigenvalues become functions of the nonlinear variational parameters: β, $\alpha(0)$, $\alpha(2)$, $\alpha(4)$, $\cdots$ (for even parity states).

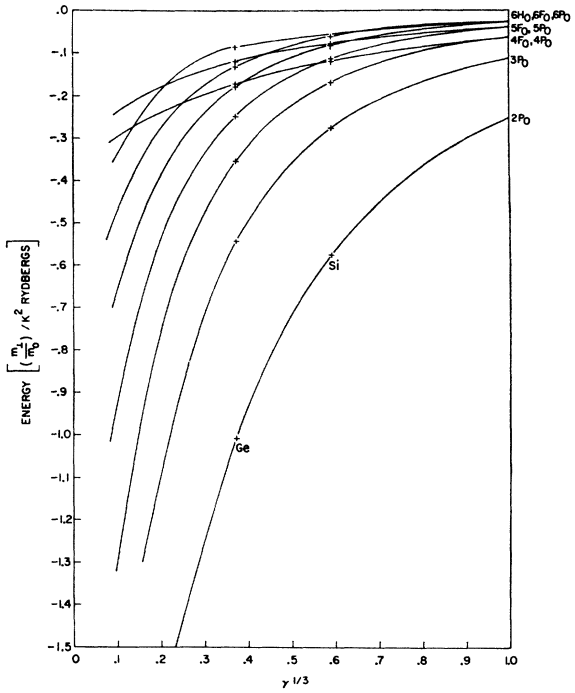

FIG. 2. P_0-like donor energy levels calculated in the effective mass approximation as functions of the mass ratio $\gamma=m_\perp/m_{||}$. The energy unit is $m_\perp e^4/2\hbar^2K^2$.

All the work is done numerically. A set of parameters (β and α's) is chosen, the Hamiltonian matrix is set up and its eigenvalues are found and the process is repeated for a new set of parameter values. Of course, one runs into the troubles of multiple minima in a multidimensional space, but these are not insurmountable. In fact, the eigenvalues displayed a remarkable constancy for a wide range of parameter values.

The numerical results to be given in the next section were obtained using the above procedure on 18 by 18 Hamiltonian matrices involving three values of l and six values of n for each l.

For the even-parity $m=0$ states (S-like), these were $l=0$, $n=1$, to 6; $l=2$, $n=3$ to 8; and $l=4$, $n=5$ to 10. For the odd parity $m=0$ or $m=\pm 1$ states (P-like), they were $l=1$, $n=2$ to 7; $l=3$, $n=4$, to 9; and $l=5$, $n=6$ to 11.

III. RESULTS

Figure 1 shows the even-parity $m=0$ energy levels (which we call S-like for convenience) as a function of the cube root of the mass ratio $\gamma=m_\perp/m_{||}$. Figure 2 shows the odd parity, $m=0$ levels, and Fig. 3 shows the odd parity, $m=\pm 1$ levels (called P_0-like and $P_\pm$-like for convenience). A small graph cannot communicate the full accuracy of the calculations, so the computed points from which the graphs are constructed are presented in Tables I, II, and III.

TABLE I. Binding energy of S-like levels (even parity, $m=0$). The energy units are ϵ_0 (Eq. 2.2) and $\gamma=m_\perp/m_\parallel$, the mass ratio. The K-L results for the $1S$ level are presented for comparison.

$\gamma^{1/3}$	0.1	0.2	0.3	0.4	0.5	0.6	0.7	0.8	0.9	1.0
$1S$	3.17	2.69	2.31	2.01	1.759	1.553	1.380	1.233	1.108	1.000
$2S$	1.88	1.29	0.928	0.695	0.541	0.437	0.366	0.3151	0.2783	0.2500
$3S$	1.21	0.79	0.545	0.394	0.297	0.234	0.190	0.158	0.1318	0.1111
$3D_0$	0.83	0.515	0.353	0.265	0.219	0.186	0.158	0.1375	0.1223	0.1111
$4S$	0.66	0.39	0.290	0.236	0.182	0.141	0.112	0.0910	0.0750	0.0625
$4D_0$	0.500	0.320	0.235	0.170	0.129	0.1045	0.0877	0.0763	0.0683	0.0625
$5S$	0.415	0.280	0.189	0.143	0.115	0.0922	0.0737	0.0596	0.0485	0.0400
$5D_0$	0.335	0.225	0.158	0.119	0.0913	0.0746	0.0632	0.0541	0.0465	0.0400
$5G_0$	0.255	0.195	0.141	0.103	0.0836	0.0679	0.0559	0.0483	0.0434	0.0400
$1S$(K-L)	3.123	2.667	2.300	2.002	1.756	1.551	1.379	1.233	1.108	1.000

TABLE II. Binding energy of P_0-like levels (odd parity, $m=0$). The energy units are ϵ_0 (Eq. 2.2) and $\gamma=m_\perp/m_\parallel$, the mass ratio. The K-L results for the $2P_0$ level are presented for comparison.

$\gamma^{1/3}$	0.1	0.2	0.3	0.4	0.5	0.6	0.7	0.8	0.9	1.0
$2P_0$	2.41	1.70	1.24	0.933	0.719	0.565	0.452	0.3663	0.3009	0.2500
$3P_0$	1.78	1.09	0.715	0.496	0.359	0.269	0.208	0.1653	0.1342	0.1111
$4P_0$	1.29	0.757	0.476	0.317	0.222	0.1618	0.1223	0.0953	0.0763	0.0625
$4F_0$	0.922	0.536	0.335	0.220	0.152	0.1157	0.0984	0.0843	0.0724	0.0625
$5P_0$	0.658	0.384	0.240	0.162	0.136	0.1087	0.0810	0.0622	0.0492	0.0400
$5F_0$	0.472	0.276	0.195	0.159	0.1095	0.0782	0.0628	0.0535	0.0461	0.0400
$6P_0$	0.338	0.238	0.174	0.116	0.0900	0.0745	0.0576	0.0439	0.0345	0.0278
$6F_0$	0.298	0.182	0.139	0.111	0.0805	0.0579	0.0449	0.0381	0.0325	0.0278
$6H_0$	0.238	0.178	0.110	0.0795	0.0645	0.0535	0.0429	0.0365	0.0317	0.0278
$2P_0$(K-L)	2.371	1.685	1.237	0.9323	0.7188	0.5650	0.4516	0.3663	0.3009	0.2500

The calculations became somewhat unstable for $\gamma^{1/3}=0.2$ and therefore the results should not be considered very accurate below this point. However, for $\gamma^{1/3}=0.3$ to 1.0, the results should be accurate to the number of digits given in Tables I, II, and III. In any case, all the computed values are strictly upper bounds to the true eigenvalues and therefore can be in error in only one direction.

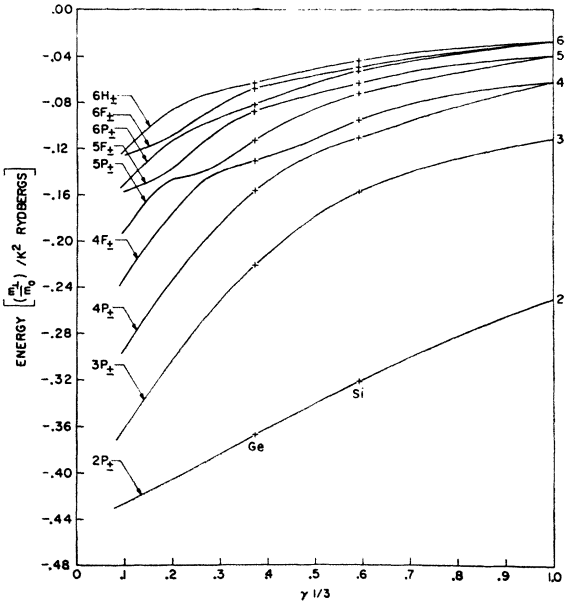

FIG. 3. $P_\pm$-like donor energy levels calculated in the effective mass approximation as functions of the mass ratio $\gamma=m_\perp/m_\parallel$. The energy unit is $m_\perp e^4/2\hbar^2K^2$.

The labeling of the energy levels according to the hydrogenic spectrum is done only for identification and to indicate the $\gamma=1$ limit for each. For any value of γ other than 1, of course, each level represents a mixture of all hydrogenic states of the appropriate parity and projection of angular momentum.

One sees in Fig. 1, and especially in Fig. 3, examples of levels attempting to cross each other. Because the levels interact, they cannot cross and one finds odd wiggles in the curves. The levels appear to cross in Fig. 2, but on an expanded scale it could be seen that they do not. Apparently, the P_0-like levels do not interact as much as the S-like or the $P_\pm$-like levels.

The method used by Kohn and Luttinger (K-L)[2] to compute the $1S$, $2P_0$, and $2P_\pm$ energy levels is identical to the present procedure applied to 1 by 1 matrices, i. e. using a single trial wave function. The K-L procedure for the $2S$ and $3P_0$ levels was to use single trial functions which had been orthogonalized to the $1S$ and $2P_0$ trial functions. The energies obtained by this latter method are not guaranteed to be upper bounds to the true eigenvalues. Nevertheless, the K-L results using the mass ratio $\gamma=0.19$ are remarkably close to those obtained in the present more elaborate calculations. Table IV shows a comparison between K-L and the present work for γ 0.19.

Figure 4 shows the K-L ground state ($1S$) energy along with the present results as a function of the mass ratio. The line marked "$\gamma\rightarrow 0$" is the asymptotic be-

TABLE III. Binding energy of $P_{\pm}$-like levels (odd parity, $m=\pm1$). The energy units are ϵ_0 [Eq. (2.2)] and $\gamma=m_\perp/m_\parallel$, the mass ratio. The K-L results for the $2P_{\pm}$ level are presented for comparison.

$\gamma^{1/3}$	0.1	0.2	0.3	0.4	0.5	0.6	0.7	0.8	0.9	1.0
$2P_{\pm}$	0.4265	0.4057	0.3835	0.3612	0.3400	0.3195	0.3002	0.2823	0.2656	0.2500
$3P_{\pm}$	0.3601	0.3025	0.2513	0.2100	0.1780	0.1548	0.1387	0.1272	0.1184	0.1111
$4P_{\pm}$	0.293	0.233	0.184	0.1470	0.1230	0.1086	0.0956	0.0832	0.0722	0.0625
$4F_{\pm}$	0.231	0.175	0.139	0.1258	0.1110	0.0936	0.0805	0.0721	0.0666	0.0625
$5P_{\pm}$	0.190	0.146	0.132	0.1055	0.0850	0.0712	0.0619	0.0538	0.0464	0.0400
$5F_{\pm}$	0.156	0.137	0.103	0.0825	0.0719	0.0622	0.0529	0.0464	0.0426	0.0400
$6P_{\pm}$	0.150	0.113	0.0925	0.0773	0.0623	0.0515	0.0443	0.0382	0.0326	0.0278
$6F_{\pm}$	0.125	0.108	0.0820	0.0639	0.0564	0.0489	0.0421	0.0367	0.0319	0.0278
$6H_{\pm}$	0.121	0.0865	0.0688	0.0600	0.0498	0.0434	0.0373	0.0324	0.0295	0.0278
$2P_{\pm}$(K-L)	0.4216	0.4026	0.3816	0.3602	0.3392	0.3191	0.3001	0.2822	0.2656	0.2500

havior of the $1S$ level as determined by K-L in the extreme adiabatic limit. It is clear from Fig. 4 that this limiting region is severely restricted to $\gamma^{1/3}<0.05$.

The $1S$, $2P_0$, and $2P_{\pm}$ states are remarkably pure for $\gamma^{1/3}>0.1$, i.e., they can be represented by a single trial wave function to a high degree of accuracy. This is evident from Fig. 4 and is borne out by an examination of the eigenvectors obtained from the diagonalization of the Hamiltonian matrix.

K-L estimated the difference between their variational results and the true eigenvalues by comparing their results and the exact values at $\gamma=0$ and $\gamma=1$, and corrected the variational results at $\gamma=0.19$ by an amount $\sim0.03\epsilon_0$. The steep slope of the extreme adiabatic limit ($\gamma\to0$) and the close agreement between the K-L "uncorrected" results and the present work for $\gamma^{1/3}>0.2$ indicate that the K-L results were closer to the exact values than they realized.

IV. APPLICATION TO EXPERIMENT

Cyclotron resonance has given the following very accurate effective mass parameters for germanium[10] and silicon[11]:

$$\text{Ge:}\quad m_\perp/m_0=0.08152\pm0.00008,\quad m_\parallel/m_0=1.588\pm0.005,\quad \gamma=m_\perp/m_\parallel=0.05134,\quad \gamma^{1/3}=0.3717;$$

$$\text{Si:}\quad m_\perp/m_0=0.1905\pm0.0001,\quad m_\parallel/m_0=0.9163\pm0.0004,\quad \gamma=m_\perp/m_\parallel=0.2079,\quad \gamma^{1/2}=0.5924.$$

TABLE IV. Comparison of K-L energy levels (Ref. 2) for the mass ratio $\gamma=0.19$ with the present work. The energy unit is ϵ_0, Eq. (2.2).

State	K-L	Present work
$1S$	−1.60	−1.600
$2S$	−0.456	−0.458
$2P_0$	−0.597	−0.600
$3P_0$	−0.288	−0.288
$2P_{\pm}$	−0.324	−0.324

Using these values of γ, the energy levels for silicon and germanium can be read from Figs. 1, 2, and 3. These energy levels are listed in Table V.

1. Silicon

One of the cleanest sets of absorption spectra published is that of phosphorus and of lithium donors in silicon[7] shown in Fig. 5. The valley-orbit splitting of the ground state of the lithium donor is only 1.8 meV and the splittings of the P-like excited states are unobservably small, indicating that the excited P-like states should be very well described in the effective mass approximation.

The spacings of the excitation lines of Li and P are listed in Table VI.

If we were to take the dielectric constant of Si to be 12.0, we would obtain a calculated separation of the $2P_{\pm}$ and the $3P_{\pm}$ levels of 2.96 meV as compared to the experimental value of 3.28 ± 0.04 meV. We observe, however, that the ratio $[E(2P_{\pm})-E(2P_0)]/[E(3P_{\pm})$

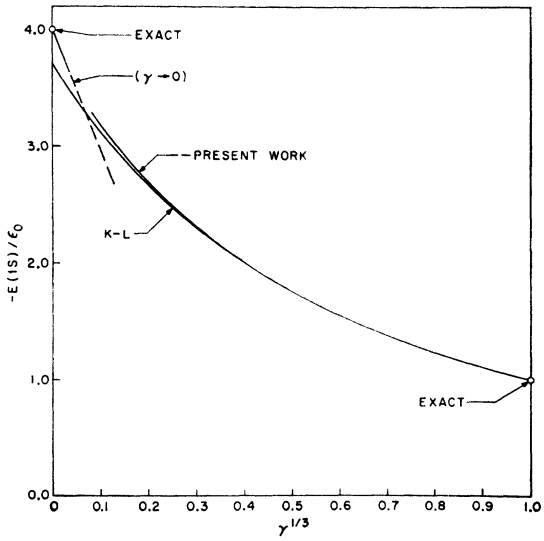

FIG. 4. Comparison of the ground-state (1S) energy of Kohn-Luttinger with the present work as a function of the mass ratio, $\gamma=m_\perp/m_\parallel$. The energy unit is ϵ_0, Eq. 2.2. The line marked "$\gamma\to0$" is the exact limiting behavior of the $1S$ level as $\gamma\to0$ (Ref. 2).

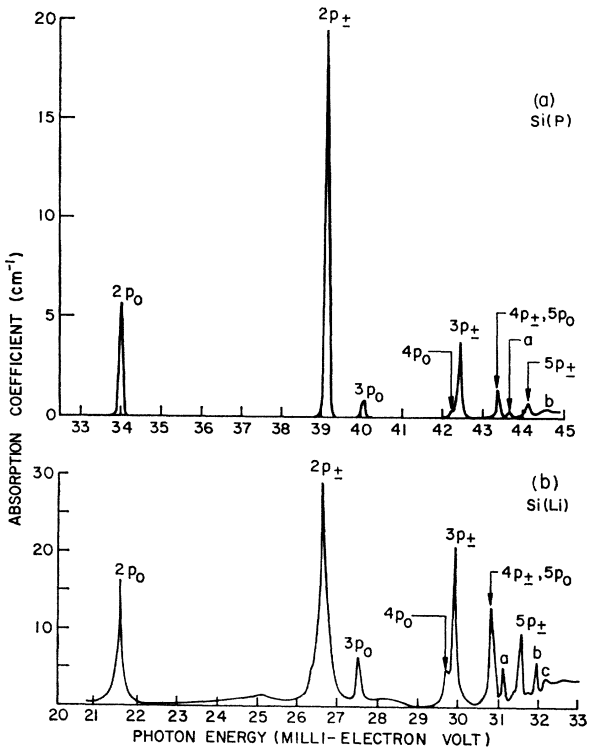

FIG. 5. (a) The excitation spectrum of the phosphorus donor in silicon; $N_0 \simeq 2\times10^{14}$ cm^{-3}. (b) The excitation spectrum of the lithium donor in silicon; $N_0 \simeq 1\times10^{15}$ cm^{-3}. Reproduced by permission from Ref. 7.

$-E(2P_\pm)]$ is independent of the dielectric constant. The theoretical value of this ratio is 1.555, and the experimental value is 1.56 ± 0.01 for Li, and 1.55 ± 0.01 for P. This close agreement between theory and experiment encourages us to question the dielectric constant. If we use the theory to determine the dielectric constant, we have

$$E(3P_\pm)-E(2P_\pm)$$
$$=0.1645\times\frac{m_l/m_0}{K^2}\times13.605 \text{ eV (theoretical)}$$
$$=3.28\pm0.04 \text{ meV (experimental)}$$

or

$$K=11.40\pm0.05$$

for the low-temperature static dielectric constant of silicon.

Using this value of the dielectric constant, we obtain the theoretical spectrum shown in Fig. 6. Also shown in Fig. 6 are the experimental spectra of Li, P, As, Sb, Bi, and the double donor, S. The previously unidentified lines called "a" and "b" in the P and Li spectra fall at $P_\pm$-like levels in the theoretical spectrum. The experimental spectra have all been arranged so that the $2P_\pm$ level in each is lined up with the theoretical $2P_\pm$ level.

TABLE V. Effective-mass binding energies of donor levels for Si ($\gamma=0.2079$) and Ge ($\gamma=0.05134$). The energy unit is meV based on $K=11.40$ for Si, and $K=15.36$ for Ge.

	$1S$	$2S$	$3S$	$3D_0$	$4S$	$4D_0$	$5S$	$5D_0$	$5G_0$
Si	31.27	8.83	4.75	3.75	2.85	2.11	1.87	1.52	1.38
Ge	9.81	3.52	2.01	1.34	1.17	0.87	0.72	0.61	0.53
	$2P_0$	$3P_0$	$4P_0$	$4F_0$	$5P_0$	$5F_0$	$6P_0$	$6F_0$	$6H_0$
Si	11.51	5.48	3.33	2.33	2.23	1.62	1.52	1.20	1.10
Ge	4.74	2.56	1.67	1.16	0.84	0.80	0.61	0.55	0.40
	$2P_\pm$	$3P_\pm$	$4P_\pm$	$4F_\pm$	$5P_\pm$	$5F_\pm$	$6P_\pm$	$6F_\pm$	$6H_\pm$
Si	6.40	3.12	2.19	1.89	1.44	1.27	1.04	0.98	0.88
Ge	1.73	1.03	0.73	0.61	0.53	0.41	0.38	0.32	0.29

The low-temperature static dielectric constant of 11.40 for Si agrees with the room-temperature long-wavelength index of refraction, $n=3.417$, measured by Salberg and Villa,[14] if the latter is reduced by the temperature coefficient

$$\frac{1}{n}\frac{dn}{dT}=(3.9\pm0.4)\times10^{-5}\text{°C}^{-1}$$

as measured by Cardona, Paul, and Brooks.[15] Aggarwal and Ramdas[9] have measured a small shift to higher energies of the excitation lines of donors in Si when the temperature of the samples is lowered. This shift can be

TABLE VI. Spacings of donor excited states in silicon. Units are meV.

States	Theory[a]	Li[b]	P[c]	As	Sb[c]	Bi[d]	S[e]	S$^+$/4[f]
$2P_\pm-2P_0$	5.11	5.13	5.06	5.12[e]	5.06	4.94	5.2	5.15
$3P_0-2P_\pm$	0.92	0.88	0.93	0.86[e]	0.95	0.93	0.7	1.08
$4P_0-2P_\pm$	3.07	3.09	3.11	2.6±0.4[g]		2.61		
$3P_\pm-2P_\pm$	3.28	3.28	3.27	3.25	3.34	3.31	3.1	3.45
$4P_0-2P_\pm$	4.07							
$5P_0-2P_\pm$	4.17	4.19	4.21	4.3±0.2[d]	4.33	4.34		4.35
$4P_\pm-2P_\pm$	4.21	4.19	4.21	4.3±0.2[d]	4.33	4.35		4.35
$4F_\pm-2P_\pm$	4.51	4.49[h]						
$5P_0-2P_\pm$	4.79							
$6P_0-2P_\pm$	4.89							
$5P_\pm-2P_\pm$	4.97	4.93	4.95	4.9±0.4[d]		5.26		
$5F_\pm-2P_\pm$	5.14							
$6F_0-2P_\pm$	5.20							
$6H_0-2P_\pm$	5.30							
$6P_\pm-2P_\pm$	5.36	5.31[h]						
$6F_\pm-2P_\pm$	5.42							
$6H_\pm-2P_\pm$	5.52							
C.B.[i]$-2P_\pm$	6.40							

[a] Theoretical values are obtained using the dielectric constant $K=11.40$.
[b] The experimental error is ±0.04 meV (Ref. 7).
[c] The energies have been adjusted where necessary to 4°K by applying a small correction due to the temperature variation of the dielectric constant. The experimental error is ±0.05 meV (Ref. 6).
[d] Experimental errors were not given for Bi (see Ref. 6, p. A609).
[e] The experimental error is ±0.5 meV (Ref. 4).
[f] These are the singly ionized sulfur double-donor levels reduced by a factor of four. Experimental error is ±0.1 meV (Ref. 4).
[g] Reference 3.
[h] These are the lines labeled "a" and "b" in the lithium spectrum. Similar lines appear in the phosphorous spectrum but their energies are not given (Ref. 7).
[i] C. B. stands for "conduction-band edge."

[14] C. D. Salberg and J. J. Villa, J. Opt. Soc. Am. 47, 244 (1957).
[15] M. Cardona, W. Paul, and H. Brooks, J. Phys. Chem. Solids 8, 204 (1959).

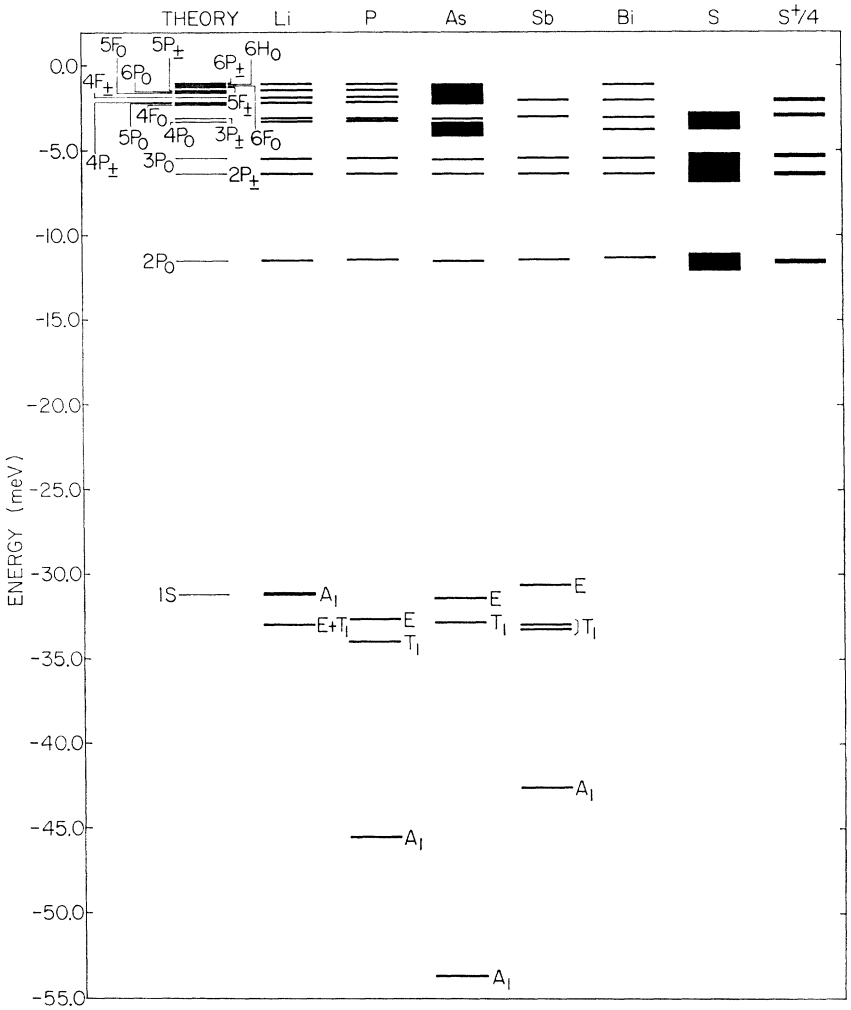

FIG. 6. Energy levels of donors in silicon. The theoretical spectrum is based on the dielectric constant appropriate for liquid-helium temperature, $K=11.40$. The experimental spectra have all been arranged so that the $2P_{\pm}$ level in each is lined up with the theoretical $2P_{\pm}$ level. The width of each level represents its experimental uncertainty, with the exception of Bi, for which no experimental error was quoted.

completely accounted for by the temperature variation of the dielectric constant.

2. Germanium

The valley-orbit splitting of the ground state of the antimony donor in germanium is only 0.32 meV[5] and, as in the silicon case, the splittings of the P-like excited states are unobservably small. We would therefore expect the P-like excited states of Sb to be quite effective-mass-like. Table VII lists the excited state energy differences.

As in the case of Si, we compute the ratio

$$\frac{E(2P_{\pm})-E(2P_0)}{E(3P_{\pm})-E(2P_{\pm})}=4.36 \quad \text{(theory)}$$

$$=4.37\pm0.05 \quad \text{(experiment)};$$

whereas, if we use 16.0 as the dielectric constant, we obtain the theoretical value of 2.78 meV for $E(2P_{\pm})-E(2P_0)$ as compared to the experimental value of (3.015 ± 0.02) meV. Proceeding as in the case of Si, we can calculate the dielectric constant which gives agreement between theory and experiment for the separation $E(2P_{\pm})-E(P_0)$ in the antimony spectrum,

$$K=15.36\pm0.05.$$

TABLE VII. Spacings of donor excited states in germanium. Units are meV.

States	Theory[a]	Sb[b]	Li[c]	P[b]	As[b]	Bi[b]
$2P_{\pm}-2P_0$	3.015	3.015	3.04	3.025	3.02	3.075
$2P_{\pm}-3P_0$	0.833	0.84	0.84	0.83	0.83	0.88
$3P_{\pm}-2P_{\pm}$	0.691	0.69	0.67	0.685	0.695	0.66
C.B.[d]$-2P_{\pm}$	1.726					

[a] Theoretical values are obtained using the dielectric constant $K=15.36$.
[b] These energies are averages of the excitation lines observed for transitions from the singlet $1S$ (A_1) ground state and transitions from the triplet $1S$ (T_1) state. The energies have been adjusted where necessary to 4°K by applying a small correction due to the temperature variation of the dielectric constant. Experimental error is ±0.02 meV (Ref. 5).
[c] Experimental error is ±0.03 meV (Ref. 7).
[d] C. B. stands for "conduction band edge."

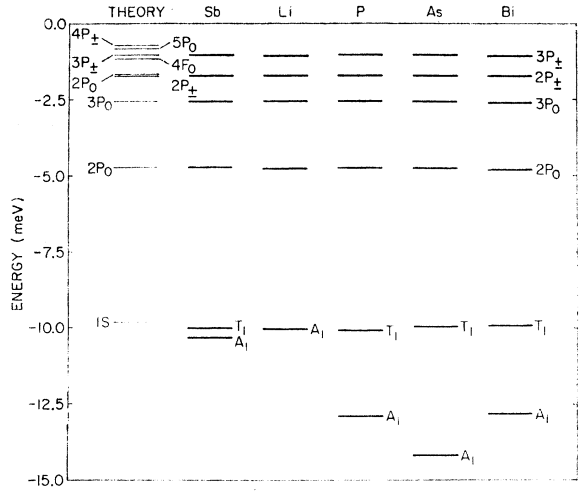

FIG 7. Energy levels of donors in germanium. The theoretical spectrum is based on the dielectric constant appropriate for liquid-helium temperature, $K=15.36$. The experimental spectra have all been arranged so that the $2P_{\pm}$ level in each is lined up with the theoretical $2P_{\pm}$ level. The width of each level represents its experimental uncertainty.

This low-temperature static dielectric constant for Ge agrees with the room-temperature long-wavelength index of refraction, $n=4.001$, measured by Salberg and Villa,[14] if the latter is reduced by using the temperature coefficient

$$\frac{1}{n}\frac{dn}{dT}=(6.9\pm0.4)\times10^{-5}\ (°C)^{-1}$$

as measured by Cardona, Paul, and Brooks.[15]

Using 15.36 as the dielectric constant, we obtain the theoretical spectrum shown in Fig. 7. Also shown in Fig. 7 are the experimental spectra of Sb, Li, P, As, and Bi. The experimental spectra have all been arranged so that the $2P_{\pm}$ level in each is lined up with the theoretical $2P_{\pm}$ level.

With this revision of the effective-mass binding energy, the experimental shift of the triplet $1S(T_1)$ state from the effective-mass value for the several donors in Ge[5] must also be revised. The new values of this shift are shown in Table VIII.

TABLE VIII. Splittings and shifts of the ground states of donors in germanium. Units are meV.

	4Δ[a]	$\Lambda-\Delta$[b]	Λ
Bi	2.87	0.11	0.83
As	4.23	0.15	1.21
P	2.83	0.26	0.97
Sb	0.32	0.20	0.28

[a] 4Δ is the splitting of the $1S$ state into the $1S$ (A_1) singlet and the $1S$ (T_1) triplet. Experimental error in 4Δ is ±0.02 meV (Ref. 5).
[b] $\Lambda-\Delta$ is the shift of the $1S(T_1)$ states below the effective-mass value.
[c] Λ is the shift of the center of gravity of the $1S$ states (A_1 and T_1) below the effective mass value.

3. Gallium Phosphide

Dean[16] has published experimental spectra of donor energy levels in GaP obtained from two-electron transitions in the decay of excitons bound to neutral donors. From the similarity of the spectra to the spectra shown in Fig. 5, he assigned the observed lines to P-like energy levels despite the parity violation this would require. Kasami[17] analyzed the spectra by computing the theoretical $2P_0$, $2P_{\pm}$, and $3P_{\pm}$ energy levels as a function of the mass ratio and fitting these three observed levels to determine the two masses and the ionization energy of the donors. He thereby determined three theoretical parameters from three pieces of data. Unfortunately, if one compares the rest of the spectrum with the theoretical levels using these parameters, there is no agreement. In fact, the experimental spectrum cannot be fit at all under the assumption that the levels are P-like. If the assumption that the levels are all S-like is adopted, one can do better, but the central-cell corrections and splittings make the interpretation far from transparent. More will be said about the situation in GaP at another time.

V. DISCUSSION

Accurate energy levels of the effective-mass Hamiltonian for donors in semiconductors with prolate-spheroid conduction-band minima have been obtained for mass ratios in the range $0.008<m_{\perp}/m_{\parallel}\leq1$. No other effects inherent in real-crystal calculations like central-cell corrections have been considered. All relativistic effects such as those discussed by Appel[18] as well as phonon interactions as treated by Nishikawa and Barrie [19,20] have been ignored.

This new determination of the effective-mass energy levels should aid in isolating true "corrections to the effective-mass formalism" from spurious ones.

The determination of new low-temperature static dielectric constants for Si and Ge in Sec. IV serves to point out again the very strong dependence of donor and acceptor energy levels on the dielectric constant. If one had an excitation spectrum of donors in a material whose mass parameters were unknown, he could use the information presented here to determine three parameters: the mass ratio, the ratio of one of the masses to the square of the dielectric constant, and the ionization limit of the spectrum. If the dielectric constant were known accurately, the masses could be obtained separately. Alternatively, as in the present work on Si and Ge, if the masses were known accurately, the dielectric constant could be determined to the accuracy of the spectrum.

[16] P. J. Dean, Phys. Rev. Letters 18, 122 (1967).
[17] A. Kasami, J. Phys. Soc. Japan 24, 551 (1968).
[18] J. Appel, Phys. Rev. 133, A280 (1964).
[19] K. Nishikawa and R. Barrie, Can. J. Phys. 41, 1135 (1963).
[20] Reference 19, p. 1823.

Note added in proof. Tefft, Bell, and Romero[21] (TBR) have recently used the same set of orthogonal functions (with minor differences in notation) as used in this work [Eq. (2.5)] to calculate effective-mass binding energies. However, TBR computed only the diagonal elements of the Hamiltonian matrix. The neglect of the off-diagonal matrix elements destroys the central principle of the variational method, namely, that the approximations to the eigenvalues are upper bounds to the true eigenvalues in a one-to-one correspondence. This becomes extremely serious when quasidegeneracies occur. Therefore, the results of TBR bear little or no relationship to the true eigenvalues of the effective-mass Hamiltonian except for the ground states of each symmetry (1S, $2P_0$, $2P_\pm$, etc.).

[21] W. E. Tefft, R. G. Bell, and H. V. Romero, Phys. Rev. **177**, 1194 (1969).

ACKNOWLEDGMENTS

The authors wish to thank J. J. Hopfield for several useful discussions on this work, and E. O. Kane and P. J. Dean for critical readings of the manuscript.

PHYSICAL REVIEW VOLUME 184, NUMBER 3 15 AUGUST 1969

Spin-Orbit Effects in Crossed Electric and Magnetic Fields; Γ_7 Band of Wurtzite-Type Crystals

KUNIICHI OHTA

I. C. Division, Nippon Electric Company, 1753, Shimonumabe, Kawasaki, Japan

(Received 9 September, 1968; revised manuscript received 18 June 1969)

The Γ_7 conduction band of the wurtzite-type II-VI compounds has a spin-orbit term linear in **k**. Effects of this spin-orbit term in crossed electric and magnetic fields are investigated on the basis of a one-band formalism. The effective Hamiltonian is solved for four different cases, according to the strength of the crossed electric and magnetic fields: (A) Strong magnetic field and weak electric field—this is essentially the simple band case; (B) weak magnetic field and weak electric field (the coupling between cyclotron motion and spin states via the spin-orbit term plays a dominant role in determining the energy spectrum); (C) strong magnetic field and strong electric field. (The major contribution to the spin-orbit interaction comes from a term representing the influence of transverse drift motion upon spin states. As a result, the spin splitting exhibits a nearly linear dependence on the electric field, and the direction of the spin axis tends toward that of the electric field with increasing electric field); (D) weak magnetic field and strong electric field [both of the spin-orbit effects, which are predominant either in the case (B) or in the case (C), are equally important, and perturbation theory is not applicable. Variational solutions have amplitudes distributed over many Landau and spin states, so that the selection rule for the intraband transitions is relaxed.] The conditions for observing these spin-orbit effects by means of intraband transitions are discussed for the actual II-VI compounds. It is found that spin-orbit effects may possibly be observed in magnetic dipole transitions under the condition of case C for CdS and ZnS, as well as in electric and magnetic dipole transitions under the condition of case A or C for CdSe. In the strong electric field of case C, the transverse drift velocity is one or two orders of magnitude larger than the velocity of sound in the crystal. Hence, phonon clouds build up around an electron to cause broadening of the resonance line. This can be avoided by carrying out the resonance experiment before the phonon clouds build up, i.e., by employing a pulsed transverse electric field.

I. INTRODUCTION

INVESTIGATION of the electronic states in crossed electric and magnetic fields has given valuable information concerning the band structure of semiconductors. The first theoretical study on this subject was made by Aronov[1] on the basis of a simple band model. The one-band effective Hamiltonian has a simple harmonic solution which can explain many qualitative features of the interband optical transitions. Later, a more appropriate theory based on a two-band model was developed by Lax and co-workers[2] and also by Aronov,[3] giving successful explanations of some critical phenomena[3,4] in the strong crossed electric field.

In the case of a complex band, however, we have to solve a set of differential equations resulting from the effective Hamiltonian.[5] The only exact solution obtained so far is the one derived by Luttinger[6] for the valence band of germanium or silicon in a magnetic field along the [111] direction with no electric field. When a weak electric field is applied perpendicular to the magnetic

[1] A. G. Aronov, Fiz. Tverd. Tela **5**, 552 (1963) [English transl.: Sov. Phys.—Solid State **5**, 402 (1963)].

[2] B. Lax, in *Proceedings of the Seventh International Conference on the Physics of Semiconductors Paris, 1964*, edited by M. Hulin (Academic Press Inc., New York, 1964), Vol. I, p. 253; B. Lax, J. Phys. Soc. Japan Suppl. **21**, 165 (1966). The latter is a review article in which an extensive list of references is given.

[3] A. G. Aronov, J. Phys. Soc. Japan Suppl. **21**, 608 (1966).

[4] W. Zawadzki and B. Lax, Phys. Rev. Letters **16**, 100 (1966).

[5] E. I. Blount, in *Solid State Physics*, edited by F. Seitz and D. Turnbull (Academic Press Inc., New York, 1962), Vol. 13, p. 306.

[6] J. M. Luttinger, Phys. Rev. **102**, 1030 (1956).